



Electrochemical Behavior of Chloroquin, Azithromycin and Hydroxychloroquin onto Carbon-Clay Paste Electrode Doped with Titanium Oxide (TiO₂)

Bakary Tigana Djonse Justin¹, Hambate Gomdje Valery^{2, *}, Zang Akono Adam Ramses¹, Niraka Blaise², Djomou Paul Nestor¹, Abdelilah Chtaini³

¹Department of Chemistry, Faculty of Sciences, University of Maroua, Maroua, Cameroon

²Department of Textile and Leather Engineering, National Advanced School of Engineering of Maroua, University of Maroua, Maroua, Cameroon

³Team of Molecular Electrochemistry and Inorganic Materials, Faculty of Sciences and Technology, University of Sultan Moulay Slimane, Beni-Mellal, Morocco

Email address:

v.hambategomdje@usms.ma (H. G. Valery)

*Corresponding author

To cite this article:

Bakary Tigana Djonse Justin, Hambate Gomdje Valery, Zang Akono Adam Ramses, Niraka Blaise, Djomou Paul Nestor, Abdelilah Chtaini. Electrochemical Behavior of Chloroquin, Azithromycin and Hydroxychloroquin onto Carbon-Clay Paste Electrode Doped with Titanium Oxide (TiO₂). *American Journal of Chemical and Biochemical Engineering*. Vol. 6, No. 1, 2022, pp. 27-35. doi: 10.11648/j.ajcbe.20220601.14

Received: May 3, 2022; Accepted: May 18, 2022; Published: May 26, 2022

Abstract: The aim of this work is to prepare and characterize a carbon-clay paste electrode doped with Titanium Oxide (CPEA/TiO₂). This electrode is used to study the electrochemical behavior of drugs such as Chloroquin, Azithromycin and Hydroxychloroquin. The morphological, structural and functional characteristics of this electrode were carried out using X-ray diffraction (XRD), selected area electron diffraction (SAED), scanning electron microscopy (SEM), Fourier transform infrared spectroscopy (FTIR). The electrochemical characterization was made by Cyclic Voltammetry (CV) in the potential range [-0.1V; 0.9V], in a phosphate buffer solution (0.1M; pH = 6.4); focused on the detection of an inorganic complex (ion [Fe(CN)₆]³⁻ (1mM)). The application was made focused on the detection of organic macromolecules such as azithromycin (AZI), chloroquin (CHL) and hydroxychloroquin (HYC). CPEA/TiO₂ was then subjected to electroanalysis in the same concentrations of the combinations AZI+CHL and AZI+HYC. However, in the presence of analyte the phenomena are irreversible with a dominance of oxidation phenomena. The electroactivity of the drugs used initially concerns the hydroxyl groups, observed around 0.050V (oxidation potential of the hydroxyl function in an intermediate form) and 0.560V (oxidation potential of the intermediate and in the carbonyl group). Secondly, the electro activity of the tertiary amine is highlighted by the potential value of 0.690V (attributable to the oxidation of the tertiary amine into an ammonium hydroxyl derivative). Current densities are more pronounced, which suggests a new molecule with significant electro activity. The oxidation mechanism is proposed. The electroactivity of the excipients (Lactose and Starch) used in these drugs is not negligible and evolves when going from one drug to two. However, the excipients are less noticeable in the AZI+HYC combination than in AZI+CHL.

Keywords: Carbon-Clay Paste Electrode, Chloroquin, Azithromycin, Hydroxychloroquin, Excipients

1. Introduction

In recent years, there has been considerable progress, especially with new technologies, the introduction of low-cost modified electrode, with high activity, low toxicity,

simple preparation, excellent resolution between peaks and a wide range of cathodic, anodic potential [1]. These modified electrodes are often used for the detection of heavy metals [2, 3], organic molecules with therapeutic properties [4].

Indeed in the era of the COVID-19 pandemic, there is a pressing need to find effective drugs to treat or prevent the

spread of the disease [5-9]. The concern about these drugs remains chloroquin and hydroxychloroquin alone or in combination with azithromycin have been studied for their clinical efficacy against COVID-19 [9]. Scientific studies have shown that over 50 years chloroquin and its structural analogue hydroxychloroquin have been used for years as drugs against malaria and certain autoimmune diseases [8]. Chloroquin has repeatedly demonstrated its ability to reduce the replication of various strains of coronaviruses in the past, including those responsible for the epidemic of severe acute respiratory syndrome (SARS) of the years 2002 and 2003 [7-9]. According to the authors, it would exert its antiviral effects by inhibiting the pH-dependent steps of the replication of several viruses, including coronaviruses. In vitro studies carried out on the strains of coronavirus responsible for COVID-19 support the potential antiviral interest of chloroquin [10] and hydroxychloroquin [11]. The results of a recent in vitro trial revealed a synergistic effect of the combination of hydroxychloroquin and azithromycin on reducing the replication of the SARS-CoV-2 virus, at concentrations compatible with those that can be obtained at the pulmonary level in humans [12]. However, the combination of these drugs has largely shown their beneficial effect in human health, but they also exert harmful effects on human health.

Indeed, in addition, significant differences were observed between chloroquin and hydroxychloroquin alone or combined with the antibiotic azithromycin for most adverse events: cardiomyopathy, cardiac arrhythmias, retinal disorders, corneal disorders, hearing disorders, headache, hepatic disorders, serious skin reactions [13]. Faced with this dilemma maintained between researchers and world politics, it is therefore important to develop methods that meet the growth in demand and allow efficient analysis and study to identify the potential safety of using these drugs against COVID-19.

These methods must be simple and sensitive, easy to implement and less expensive, while allowing the determination of the electrochemical behavior of these drugs. It is in this context that electrochemical techniques offer an interesting alternative because they make it possible to achieve high sensitivities, stability and selectivity, they are inexpensive and easily adaptable to miniaturization and portable [14] and are widely studied in the literature given their possible applications in different fields such as aeronautics, medicine, automotive, solar energy [15].

The aim of this work is to develop a carbon-clay paste electrode doped with titanium oxide, as a new low-cost material. It is used to study the electrochemical behavior of drugs such as chloroquin, azithromycin and hydroxychloroquin by cyclic voltammetry and finally proposed a possible reaction mechanism.

2. Material and Methods

2.1. Material and Chemicals Reagents

The clay material used in this work was the subject of previous work [2]. The reagents used in this work are

analytically reliable, therefore have not undergone any prior purification. The binder used (paraffin oil), titanium oxide and [Fe(CN)₆]³⁻ are purchased from Sisco Research Laboratories pvt. Ltd, India. Phosphate buffer solution (0.1 M, pH=6.4) was prepared with KH₂PO₄ and K₂HPO₄ (Riedel-de-Haën) and used as the supporting electrolyte. Chloroquin, Azithromycin and Hydroxychloroquin have been used in the pharmaceutical form. The carbon graphite powder was prepared from battery residues and the purification method adopted is described in previous work [16].

2.2. Characterization Techniques

Information regarding the morphology of modified carbon paste powder was achieved by using a Hitachi (Japan) S-3000H electron microscope at an accelerating voltage of 15 kV which was performed using carbon tape. The absorption bands of modified electrodes were performed using FT-IR by using the KBr method in which pellet were homogenized by grinding of powder mixture of KBr and MSB, hard-pressed using SHIMADZU MHP-1 hand press. The measurements recorded in IR range of 400-4000 cm⁻¹ with 45 scan which was done with the aid of SHIMADZU 8400S FT-IR instrument. In order to determine the mineralogical composition of modified electrode, X-ray diffraction of material powder were recorded using Bruker D8 Advance X-ray diffractometer with Cu K α ($\lambda = 1.5405 \text{ \AA}$) radiation at diffraction angle of 2θ between 10 - 50°. Selected Area Electron Diffraction (SAED) of modified electrode was taken with a Tecnai F20 (FEI) transmission electron microscope with an accelerating voltage of 200 kV.

Electrochemical measurements were performed in cells equipped with three electrodes using a Pgstat-12 Autolab potentiostat/galvanostat driven by general electrochemical systems for computer data processing (Volta lab. master 4 software). A three-electrode system composed of carbon-clay doped with titanium oxide was used as the working electrode, a silver chloride electrode as the reference electrode, and a platinum wire was used as the counter electrode.

2.3. Preparation of the Working Electrode

The working electrode used in this work is a carbon-clay paste electrode doped with titanium oxide (CPEA/TiO₂) which will be produced by mixing a powder of graphite, clay, titanium oxide and paraffin oil (binder) in a two-step procedure. The CPEA/TiO₂ electrode is prepared by manually mixing clay powder and graphite powder in a mass ratio of 50%-50% and 30% of TiO₂. Paraffin oil will then be added drop by drop while stirring until a paste is obtained. Ethanol at the end will be added to the mixture in an appropriate amount as an inert volatile solvent and the resulting mixture will be well homogenized, then left in the air for the evaporation of the solvent. The paste is manually inserted into the cylindrical cavity of the electrode body (geometric surface of the working electrode is approximately 0.25cm²).

The protocol for the electrochemical detection of organic compounds used in this work is generally based on three

phases: the open circuit accumulation phase of the organic compounds in a soiled aqueous medium on the surface of the working electrode, the detection phase and the desorption phase. In the experiment, two approaches are possible, the case where the accumulation and the detection take place in the same medium and the case where the accumulation and the detection take place in two different mediums.

3. Results and Discussion

3.1. Structural and Mineralogical Analysis of the Modified Electrode

Analysis by X-ray diffraction (XRD) as presented in figure 1 shows that the graphite is well crystallized and presents a single intense line at 27° (interlayer distance: 3.4 \AA) corresponding to the reticular plane (002) graphitic carbon [17]. The peak centered on the 25.31° position in 2θ is characteristic of the (101) TiO_2 line of the anatase phase [18]. Quartz (Q) was observed 2θ equals 26. We also note that at 2θ equals 36 and 41 attributed to the presence of Kaolinite (K). A peak which appears around a value of 2θ equals 12.5 and 54.6 equivalents according to the Bragg relation of the characteristic diffraction peaks attributed to Montmorillonite (Mt). This result is confirmed by the SAED which shows that the modified electrode consists of several particles arranged in the form of layers.

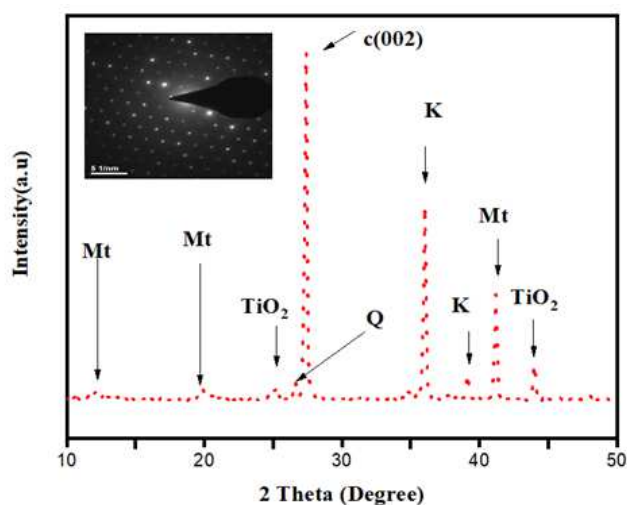


Figure 1. Diffraction pattern and selected area electron diffraction (SAED) of CPEA/ TiO_2 .

3.2. Functional Analysis of the Modified Electrode

The materials were analyzed by infrared spectroscopy (Figure 2). The IR spectrum of CPEA/ TiO_2 presents a vibration band around 3612 cm^{-1} which can be attributed to the hydroxyl group (O-H) [19]. The band at 3703 cm^{-1} is characteristic of the Ti-OH vibration [18]. The vibration band observed at 1640 cm^{-1} is characteristic of the ethylenic double bond ($\text{C}=\text{C}$) [18, 19]. As for the band at 1030 cm^{-1} , it accounts for the stretching vibration of the Si-O bond in the tetrahedral layer. In addition, the band at 918 cm^{-1}

materializes the Si-O-Ti bonding vibrations. Ultimately, the band around 505 cm^{-1} provides information on the strain vibration of Si-O-Al bonds.

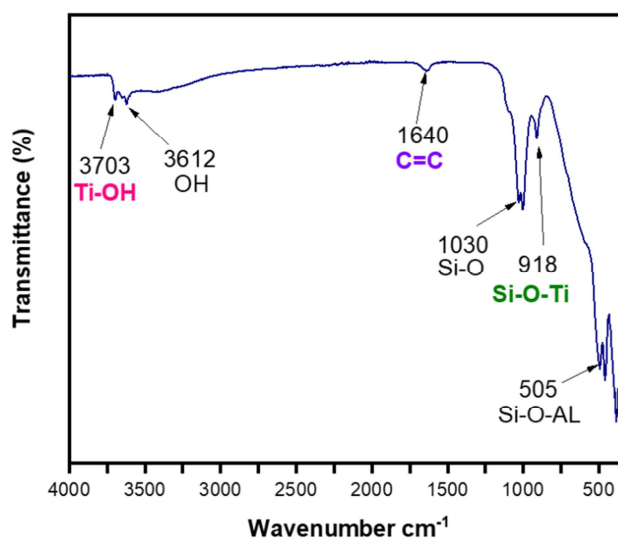


Figure 2. Spectra of the FTIR analysis of CPEA/ TiO_2 .

3.3. Morphological Analysis of the Modified Electrode Surface

Figure 3 below shows the morphology of the modified electrode, it shows an agglomerate of particles of various sizes arranged with a graphitic structure composed of slips. The presence of particles of hexagonal shapes can testify to Quartz crystals.

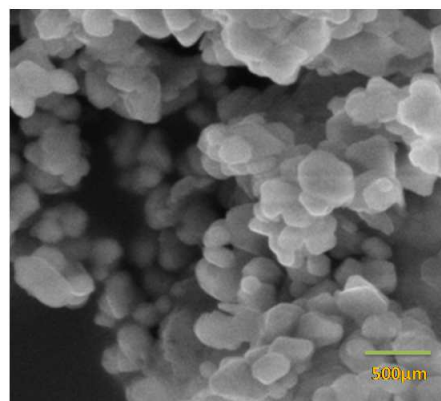


Figure 3. Scanning electron microscopy image of the surface of CPEA/ TiO_2 .

3.4. Electrochemical Characterizations

3.4.1. Electro Activity of the Carbon-Clay Paste Electrode Doped with Titanium Oxide in a Phosphate Buffer Solution (0.1M; pH=6.4)

In order to evaluate the reproducibility of the CPEA/ TiO_2 electrode, the latter was characterized by cyclic voltammetry (45 cycles) in the potential range $+0.8$ and -0.1 V in a buffer medium. Figure 4 below is an illustration. It emerges that as the cycles follow one another, the voltammograms seem to converge towards a standard form, proof that the

electrochemical phenomena are reproducible with respect to the proposed working electrode. Previous work [20] report similar behavior. At the interval of the chosen potential, no oxido-reduction phenomenon is perceptible on the surface of the modified electrode. The different voltammograms are stable and reproducible [21, 22] showing the electroactive nature of CPEA/TiO₂.

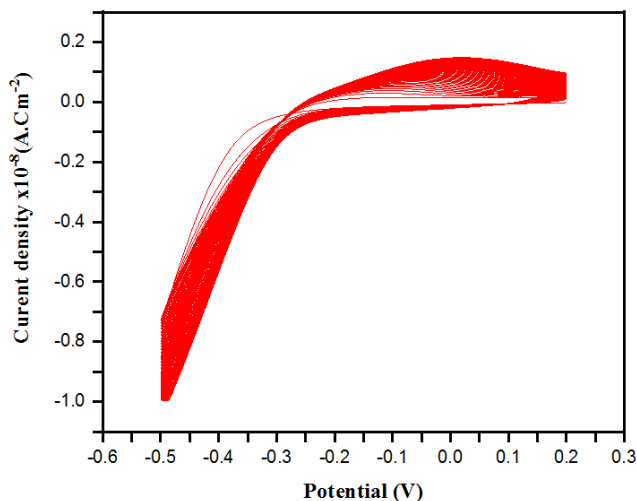


Figure 4. CV's recorded in electrolytic solution of phosphate buffer (0.1M; pH=6.4) on CPEA/TiO₂ at the scan rate $V = 50$ mV/s.

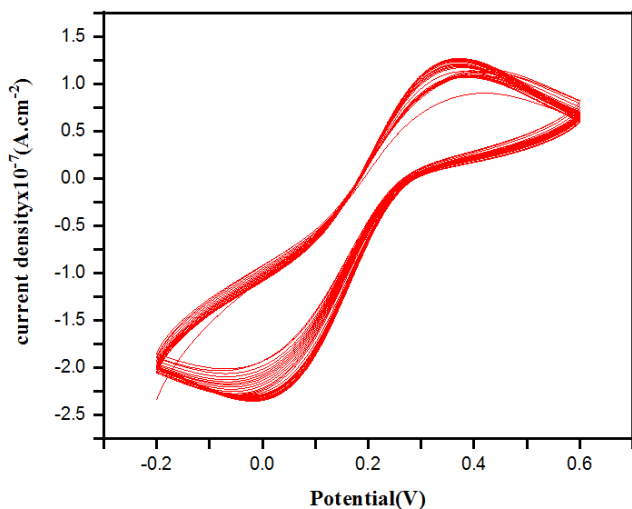


Figure 5. CV's recorded for a solution containing $[Fe(CN)_6]^{3-}$ (1mM) ions on CPEA/TiO₂ in electrolytic solution of phosphate buffer (0.1M; pH=6.4) at the scan rate $V = 50$ mV/s.

3.4.2. Electro Activity of the Carbon-Clay Paste Electrode Doped with Titanium Oxide in the Presence of $[Fe(CN)_6]^{3-}$ Ions

Figure 5 shows the application of CV's for the collection of information about the porosity and the permselectivity properties of CPEA/TiO₂ [20].

After 5 min of preconcentration in open circuit, the electrochemical measurements were made upon multisweep (45 cycles) when the supporting electrolyte contains $[Fe(CN)_6]^{3-}$ (1mM) ions by CV's in the potential range between + 0.8 and - 0.1 V, stable voltammograms are

obtained. According to figure 5, the redox phenomena are reversible because the CV's are symmetric between the anodic and cathodic peaks. The mean current density is 0.141×10^{-8} A.cm⁻² for CPEA/TiO₂ in absence of $[Fe(CN)_6]^{3-}$. In presence of $[Fe(CN)_6]^{3-}$, the current density peak (1.250×10^{-7} A.cm⁻²) materialize the oxidation of $[Fe(CN)_6]^{4-}$ ions [20]. The current density peak around -2.345×10^{-7} A.cm⁻² are attributable to the reduction of $[Fe(CN)_6]^{3-}$ ions to $[Fe(CN)_6]^{4-}$ [21].

3.5. Application

3.5.1. Electrochemical Behavior of Chloroquin, Azithromycin and Hydroxychloroquin Molecules

(i). Electrochemical Behavior of Azithromycin on CPEA/TiO₂

Figure 6 below shows the study of the behavior of the CPEA/TiO₂ electrode (electrochemical behavior of azithromycin) by cyclic voltammetry in a phosphate buffer medium (0.1M; pH=6.4), in the potential interval [+0.8; - 0.1]. It emerges that this electrode is electroactive in the presence of azithromycin because the cyclic voltammetric measurement shows three anodic peak of currents densities, 2.975×10^{-8} A.cm⁻² corresponding to the oxidation of the hydroxyl group into an intermediate [23, 24], 17.430×10^{-8} A.cm⁻² materializing the oxidation of the intermediate into a terminal carbonyl group (C=O) [23] and 18.440 A.cm⁻², corresponding to the oxidation of the tertiary amine function into an ammonium hydroxyl derivative. The CV of Figure 6 shows also that the electrode is more favorable to oxidation phenomena (presence of two peaks) than reduction phenomena. This behavior could be explained by the fact that the massive presence of heteroatoms in the molecule studied confers on the latter a great nucleophilic power. According to the mechanism of electro-detection of Azithromycin (figure 7), the oxidation phenomenon concerns more the less crowded hydroxyl and amine groups.

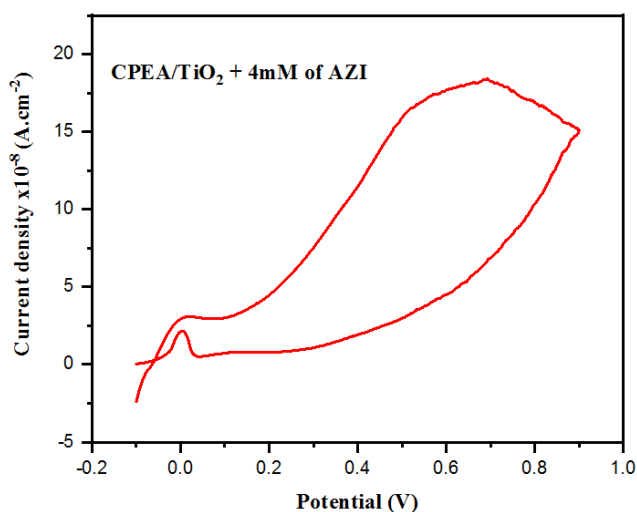


Figure 6. CV recorded by CPEA/TiO₂ in presence of 4mM azithromycin in electrolytic solution of phosphate buffer (0.1M; pH=6.4) with a scan rate of 50 mV/s.

The following Mechanism is proposed:

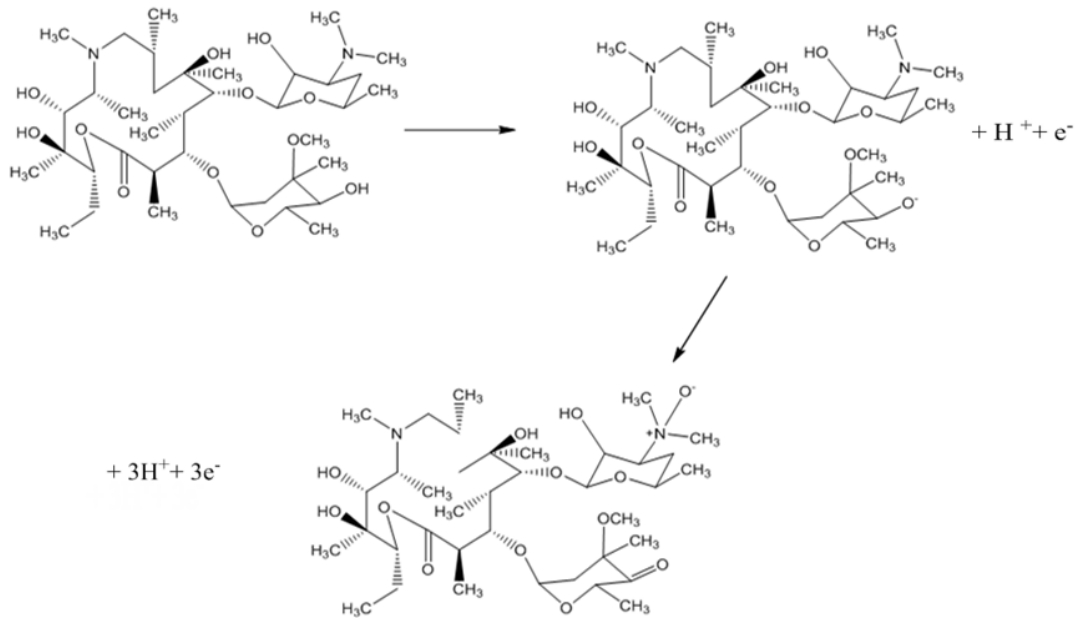


Figure 7. Azithromycin oxidation mechanism.

(ii). Electrochemical Behavior of Hydroxychloroquin on CPEA/TiO₂

The ability of the modified electrode to recognize hydroxychloroquin was studied by CV under the same conditions as before (see figure 8). It also emerges with this other molecule (hydroxychloroquin) that the electroactivity of the electrode remains preserved with regard to peak current density. The related voltammogram shows the presence of two anodic peaks of current densities, one of which around 14.027 A.cm⁻² corresponding to the oxidation of the alcohol function and the other around 2.444 A.cm⁻² could correspond to the oxidation of the hydroxyl group into an intermediate (figure 9) by agreeing with the work of Raja and Chtaini [24]. In addition, the voltammogram in Figure 8 below shows that the oxidation-reduction phenomena of hydroxychloroquin are irreversible at the surface of the proposed working electrode, under the conditions of the experiment. Figure 9 below shows the mechanism of oxidation of hydroxychloroquin on the surface of the modified electrode.

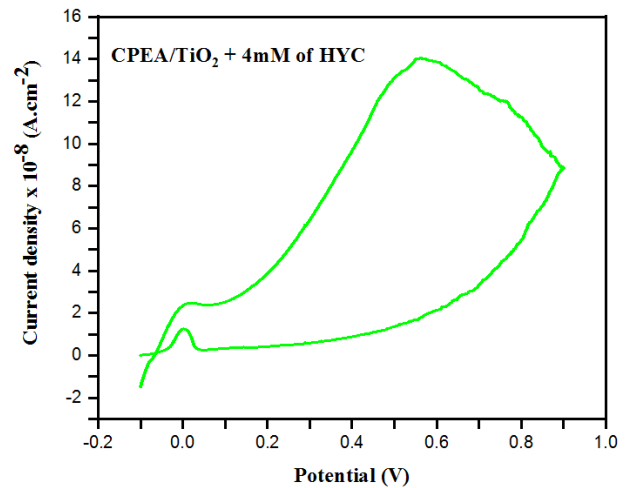


Figure 8. CV recorded by CPEA/TiO₂ in presence of 4 mM hydroxychloroquin in electrolytic solution of phosphate buffer (pH=6.4) with a scan rate of 50 mV/s.

The Following mechanism of oxidation is proposed:

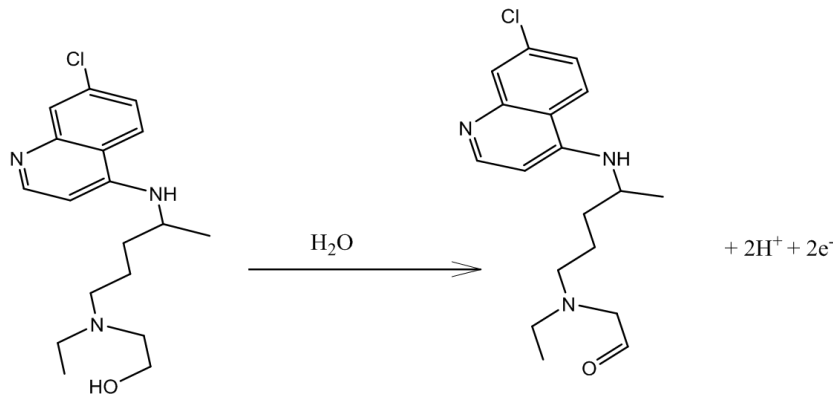


Figure 9. Mechanism of oxidation of hydroxychloroquin.

(iii). Electrochemical Behavior of Chloroquin on CPEA/TiO₂

Figure 10 below shows the electro analysis of chloroquin in the presence of the modified electrode. Electrochemical measurements were made by cyclic voltammetry, under similar conditions as before. The intense anodic peak of current density ($3.880 \times 10^{-7} \text{ A.cm}^{-2}$) corresponding to the 0.690V potential is attributable to the oxidation of the amine tertiary to an ammonium hydroxyl derivative. The oxidation of the secondary amine function is not observed as in the work of Lam *et al.* [25] because the potential range used (-0.1 to -0.9V) in the case of this work does not allow it. The anodic potential around 0.020V could be attributed to the excipients such as lactose and starch used in the formulation of the medication [26]. Figure 11 below also shows that the electrode is more favorable to oxidation reactions due to its high nucleophilic power.

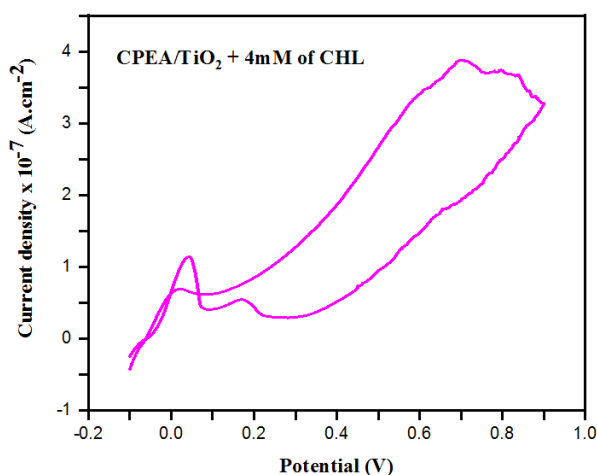


Figure 10. CV recorded by CPEA/TiO₂ in presence of 4 mM chloroquin in electrolytic solution of phosphate buffer (0.1M; pH=6.4) with a scan rate of 50 mV/s.

The Mechanism proposed is:

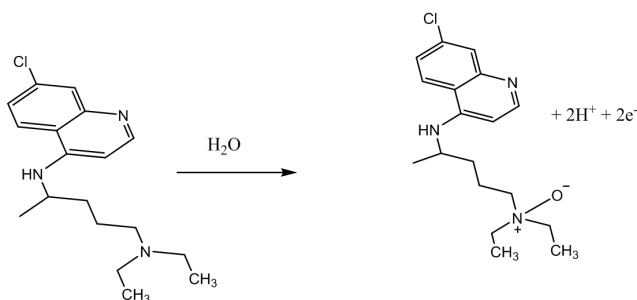


Figure 11 Chloroquin oxidation mechanism.

3.5.2. Interference Effect of Different Molecules

The combination of the different drugs are used in the treatment of COVID-19, the electrochemical analysis of the combination of these drugs will better elucidate their electrochemical behavior in a buffer medium. Figure 12 below is an illustration. Under conditions where the

different analytes have the same concentrations (4mM) in a 0.1M phosphate buffer solution (0.1M) and pH=6.4, the CV's recorded make it possible to distinguish in the direction of the anodic scan four peaks P₁, P₂, P₃ and P₄ appearing respectively at potentials 0.070 V, 0.220V, 0.560V and 0.690V. The P₄ peak corresponds to the oxidation of the tertiary amine function to an ammonium hydroxyl derivative, while that P₃ is attributable to the oxidation of the intermediate (figure 11) to a carbonyl group. The P₂ peak would materialize the oxidation of the AZI and CHL excipients (Lactose and Starch). The P₁ peak is ultimately attributable to convert through the intermediate (figure 11) in the two drugs put together [24].

It is important to note that during the electroanalysis of azithromycin alone, the anodic scan showed a peak current of the order of $3.120 \times 10^{-8} \text{ A.cm}^{-2}$ for a potential of 0.020V corresponding to oxidation hydroxyl group to an oxidized intermediate form (figure 11). In addition, the oxidation of the excipient was not materialized on the related voltammogram. With chloroquin alone, on the other hand, the excipient was identified at the potential of 0.020V for an anode peak current density of $6.900 \times 10^{-8} \text{ A.cm}^{-2}$. By combining the drugs AZI and CHL, it is clear that not only the oxidation of the excipient is materialized but, this phenomenon requires a higher potential (0.020V to 0.220V). This change in potential value could be attributed to a reaction between the excipients resulting from the two drugs. Furthermore, the peak current density relating to the oxidation of excipients increases from $6.900 \times 10^{-8} \text{ A.cm}^{-2}$ (in CHL alone) to $2.070 \times 10^{-7} \text{ A.cm}^{-2}$ (in the mixture of the two drugs), proof that the combination of the two drugs is likely to boost its electrochemical activity [27].

Figure 12a shows not only that the first oxidation (giving rise to the intermediate) experiences a slight shift in the positive direction (0.020V to 0.060V) but the related peak current density is very pronounced ($2.460 \times 10^{-7} \text{ A.cm}^{-2}$) compared to that found in the case of electroanalysis of AZI alone ($3.12 \times 10^{-8} \text{ A.cm}^{-2}$). This increase in current density at the electrode surface accounts for the increase in affinity between the mixture of the two drugs and the modified electrode surface. This increase would be due to reactions between the two molecules in the electrolyte solution [28].

As for the characteristic oxidation potentials of the intermediate in the carbonyl group (0.560V) and that of the oxidation of the tertiary amine function (0.690V), they remain unchanged. It goes without saying that they behave like fingerprints for AZI and CHL molecules.

Figure 12b presents the electrochemical activity of the combination of AZI and HYC. As a result, the anodic scan reveals three peaks, namely P₁ (0.090V; $3.400 \times 10^{-7} \text{ A.cm}^{-2}$), P₂ (0.180V; $1.350 \times 10^{-7} \text{ A.cm}^{-2}$) and P₃ (0.690V; $1.670 \times 10^{-7} \text{ A.cm}^{-2}$). The P₁ peak is attributable to the oxidation of the hydroxyl. The peak P₂ materializes the oxidation of the excipients while the peak P₃ corresponds to the oxidation of the tertiary amine to an ammonium hydroxyl derivative. The peak materializing the oxidation of the carbonyl intermediate

is inhibited by the other functions during the anodic scan.

If the potentials materializing the excipients in the AZI+CHL (figure 12a) and AZI+HYC (figure 12b) formulations are identical (0.200V), this is not the case for the current densities. Indeed, with the AZI+CHL combination, this density is of the order of $2.060 \times 10^{-7} \text{ A.cm}^{-2}$ whereas with the AZI+HYC combination, it is rather $1.350 \times 10^{-7} \text{ A.cm}^{-2}$. This low value obtained with AZI+HYC shows that it is of greater interest to use AZI+HYC to the detriment of AZI+CHL because the excipients not being the active principles of the drugs, a great electrochemical activity of those this would minimize the expected results.

Figure 12b further shows that the first oxidation of the hydroxyl group takes place at a slightly higher potential than

that obtained with AZI+CHL (0.090V against 0.060V). It goes without saying that the AZI+HYC association requires a greater potential difference. By observing the current density corresponding to this oxidation ($3.400 \times 10^{-7} \text{ A.cm}^{-2}$), it is clearly higher than the values found both with AZI alone ($3.120 \times 10^{-8} \text{ A.cm}^{-2}$) than with the AZI+CHL combination ($2.460 \times 10^{-7} \text{ A.cm}^{-2}$). The high current density obtained during the first oxidation of the hydroxyl group with the combination AZI+HYC shows that the modified electrode is more electroactive with respect to AZI+HYC than with AZI alone or with AZI+CHL. These results show that the interaction between the molecules of azithromycin and hydroxychlorin are more important due to the functional groups present in the two molecules [28-30].

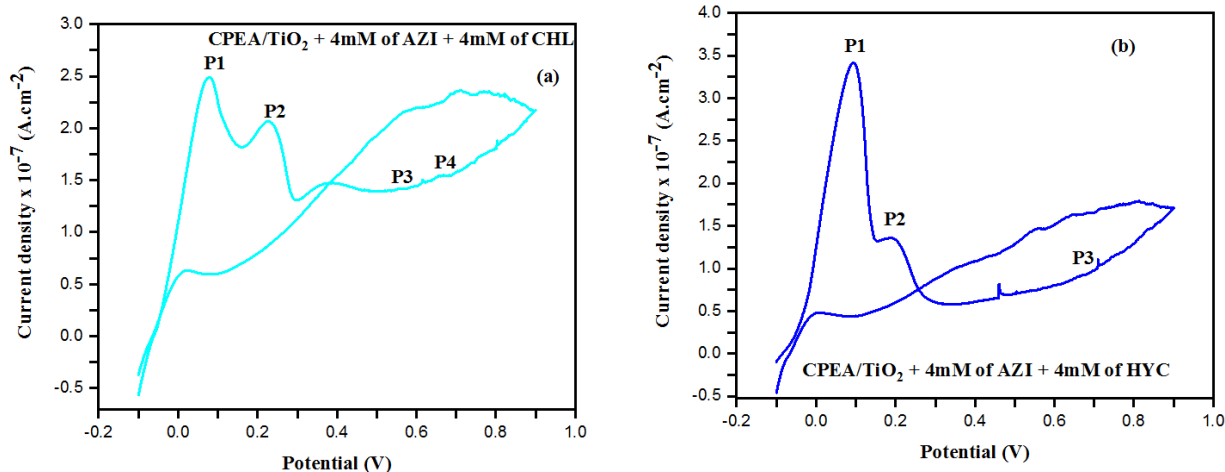


Figure 12. CV's recorded by CPEA-TiO₂ in electrolytic solution of Phosphate buffer (pH=6.4), at scan rate of 50 mV/s. (a) CHL (4mM) +AZI (4mM) and (b) HYC (4mM) +AZI (4mM).

4. Conclusion

The electro activity of a carbon paste electrode modified with clay and doped with titanium oxide (TiO₂) was studied by cyclic voltammetry in a phosphate buffer medium. The proposed working electrode (CPEA/TiO₂) is electroactive in the buffer solution used. The sensitivity, reproducibility, selectivity and stability of this electrode is studied. Inorganic complex ions ([Fe(CN)₆]³⁻) and organic macromolecules (AZI, CHL and HYC) are used as test samples. By subjecting the CPEA/TiO₂ electrode to the combinations AZI+CHL on the one hand and AZI+HYC on the other hand, its intrinsic selectivity was brought to the surface.

The electrochemical behavior of each drug is studied at the surface of the CPEA/TiO₂ electrode and also in a combined manner. It appears that the current density is more increasing when azithromycin is associated with hydroxychlorin, which can be explained by the interactions between the two molecules.

Conflicts of Interest

All the authors do not have any possible conflicts of interest.

Acknowledgements

The outcome of this work finds satisfaction in the support granted by the Analytical Chemistry Laboratory of the University of Yaoundé I (Cameroon), the Council for Scientific and Industrial Research (CSIR), the World Academy of Sciences for Advancement of Science in Developing Countries (TWAS) and the Analysis Center of the Faculty of Science and Technology of the Sultan Moulay Slimane University of Beni-Mellal (Morocco).

References

- [1] Peik-See, T., Pandikumar, A., Nay-Ming, H., Hong-Ngee, L., 2014. Simultaneous Electrochemical Detection of Dopamine and Ascorbic Acid Using an Iron Oxide/Reduced Graphene Oxide Modified Glassy Carbon Electrode, *Sensors Basel*. 14, 15227-15243.
- [2] Niraka, B., Hambate, G. V., Raja, M., Mohamed, O., Bakary, T. D. J., Edwin, A. O., Abdelilah, C., 2022. Simultaneous Electrochemical Detection of Pb and Cd by Carbon Paste Electrodes Modified by Activated Clay, *Journal of Analytical Methods in Chemistry*, Article ID 6900839.

- [3] Touzara, S., Najih, R., Abdelilah, C., 2016. Electrochemical Sensor Based on 2-Benzimidazolethiole Modified Carbon Paste Electrode for Lead Chelation Therapy, *Journal of Biomolecular Research & Therapeutics*. 5, 1000137.
- [4] Xavier, B. J., Sriram, W. B., Sea-Fue., Baby, J. N., Yung-Fu, H., Mary, G., 2021. Revealing the effect of multidimensional ZnO@CNTs/RGO composite for enhanced electrochemical detection of flufenamic acid, *Microchemical Journal*. 168, 106448.
- [5] Amir, S., Brian, C., Henriksen, H., Joshua, B. D., 2020. Safety signals for QT prolongation or torsades de pointes associated with azithromycin with or without chloroquine or hydroxychloroquine. 17, 483- 486.
- [6] Pastick, K. A., Fan Wang., Sarah, L. M., Skipper, C. P., Matthew, P. F., Radha, R., 2020. Review: Hydroxychloroquine and Chloroquine for Treatment of SARS-CoV-2 (COVID-19), *Infectious Diseases Society of America*. 7, 32363212.
- [7] Million, M., Lagier, J. C., Gautret, P., Colson, P., Fournier, P. E., Fenollar, P., Brouqui, Didier, R., 2020. Early treatment of COVID-19 patients with hydroxychloroquine and azithromycin: A retrospective analysis of 1061 cases in Marseille, France. *Travel medicine and infectious disease*. 35, 101738.
- [8] Christian, D. A., Rolain, J. M., Philippe, C., Didier, R., 2020. New insights on the antiviral effects of chloroquine against coronavirus: what to expect for COVID-19, *International Journal of Antimicrobial Agents*. 55, 105938.
- [9] Papazisis, G., Siafis, S., Cepatyte, D., Giannis, Stamoula, E., Tzachanis, D., Egberts, T., 2020. Safety profile of chloroquine and hydroxychloroquine: an analysis of the FDA Adverse Event Reporting System (FAERS) database. 25, 6003-6012.
- [10] Kapoor, A., Pandurangi, U., Arora, V., Gupta, A., Jaswal, A., Nabar, A., Naik, A., Naik, N., Namboodiri, N., Vora, A., 2020. Cardiovascular risks of hydroxychloroquine in treatment and prophylaxis of COVID-19 patients: A scientific statement from the Indian Heart Rhythm Society. *Indian Pacing Electrophysiol. J*. 20, 117-120.
- [11] Gautret, P., Lagier, J. C., Parola, P., Hoang, V. T., Meddeb, L., Mailhe, M., Doudier, B., Courjon, J., Giordanengo, V., Vieira, V. E., 2020. Hydroxychloroquine and azithromycin as a treatment of COVID-19: results of an open-label non-randomized clinical trial. *International journal of antimicrobial agents*. 56, 105949.
- [12] Yao, X., Ye Ye, F., Zhang, M., Cui, C., Huang, B., Niu, B., Liu, X., Zhao, L., Dong, E., Song, C., Zhan, R., Lu, H., Tan, W., Liu, D., 2020. In Vitro Antiviral Activity and Projection of Optimized Dosing Design of Hydroxychloroquine for the Treatment of Severe Acute Respiratory Syndrome Coronavirus 2 (SARS-CoV-2). *Clinical infectious diseases: an official publication of the Infectious Diseases Society of America*. 71, 732-739.
- [13] Wang, M., Cao, R., Zhang, L., Yang, X., Liu, J., Xu, M., 2020. Remdesivir and chloroquine effectively inhibit the recently emerged novel coronavirus (2019-nCoV) in vitro. *Cell research*. 30, 269-271.
- [14] Hambate, G. V., Abdelilah, C., Loura B., 2019. Voltammetric Sensor Based on Electrodes Modified by Poly (vinyl alcohol)-Natural Clay Film, for the Detection of Gallic Acid *Portugaliae Electrochimica Acta*. 37, 327-333.
- [15] Ennachete, M., Saâdane, H., El Mastour, J., El Quatli, S. E., Hambate, G. V., Abdelilah, C., 2019. Electrochemical sensor based on the carbon paste electrode modified with polymer for determination of copper ions, *World Journal of Pharmacy and Pharmaceutical Sciences*. 8, 97-107.
- [16] Tegua, D. R., Noumi, G. B., Domga., 2021. Dip Coating deposition of Manganese oxide nanoparticles on graphite by sol gel technique for the indirect electrochemical oxidation of methyl orange dye: Parameter's optimization using box-behken design. *Case Studies in Chemical and Environmental Engineering*. 3, 100068.
- [17] Rashed, A. E., El-monein, A. A., 2017. Two steps synthesis approach of MnO₂/graphite composite electrode for supercapacitor application. *Mater Today Energy*. 3, 24-31.
- [18] Yao, Y. W., Cui, L. H., Li, Y., Yu, N. C., Dong, H. S., Chen, X., Wei, F., 2015. Electrocatalytic Degradation of Methyl Orange on PbO₂-TiO₂ Nanocomposite Electrodes. 9, 1357-1364.
- [19] Inna, S., Jiokap, N. Y., Tsamo, C., Dinica M. R., Kamga, R., 2019. Influence of physico-chemical parameters on fuel briquettes properties formulated with mixture of biomasses, *J. Env. Sci. Pollut. Res*. 5, 338-341.
- [20] Tonle, K. I., Ngameni. E., Tchieno, M. F., Walcarius, A., 2015. Organoclay-modified electrodes: preparation, characterization and recent electroanalytical Applications, *J Solid State Electrochem*. 19, 1949-1973.
- [21] Dai-yang, L., Pengou, M., Tcheumi, L. H., Dawai, N., Wahabou, A., Ngana, N. B., Ngameni., 2020. Emmanuel, Physico-Chemical and Electrochemical Characterizations of a Trachyte in the Far North Region of Cameroon for Possible Electroanalytical and Environmental Purposes. *Journal of Inorganic and Organometallic Polymers and Materials*. 31, 542-551.
- [22] Kemmegne, M. J. C., Toma, E. H., Araki, K., Vera, R. L. C., Ngameni. E., 2016. Simultaneous determination of acetaminophen and tyrosine using a glassy carbon electrode modified with a tetraethenated cobalt (II) porphyrin intercalated into a smectite clay, *Springer-Verlag Wien*. 183, 3243-3253.
- [23] Rebelo, P., Pacheco, J. G., Cordier, M. N. D. S., Melo, A., Delerue-Matos, C., 2020. Azithromycin electrochemical detection using a molecular imprinted polymer prepared on a disposable screen-printed electrode This journal is The Royal Society of Chemistry. 11, 216455026.
- [24] Raja, M., Abdelilah, C., 2019. Biomaterials Electrodes for Degradation of Phenol Anal. *Bioanal. Electrochem, Anal. Bioanal. Electrochem*. 11, 1206-1216.
- [25] Zhao, X., Liu, X., Baoyu, H., Pu, W., Yong, P., 2019. Hydroxyl group modification improves the electrocatalytic ORR and OER activity of graphene supported single and bi-metal atomic catalysts (Ni, Co, and Fe), *J. Mater. Chem*. 7, 24583.
- [26] Lam, K., Van Wyck, S., 2017. Geiger, W. E., One-electron oxidation of chloroquine, cymanquine, and related aminoquinolines in nonaqueous media, *Journal of Electroanalytical chemistry*. 799, 531-537.
- [27] Vajdle, O., Guzsány, V., Škoric, D., Csanád, J., Milos, P., Milka, A., Zoltán, K., Petrovic, S., Andrzej, B., 2017. Voltammetric behavior and determination of the macrolide antibiotics azithromycin, clarithromycin and roxithromycin at a renewable silver-amalgam film electrode *Electrochimica Acta*. 229, 334-344.

- [28] Pirnay, G., Billal, D., Tourid, W., Amel, T., Fatima, B., Leila, N., Nadia, A., Walid, A. Zakya, A., Ayhan, B., Marie-Line, G. D., Aikpa, R, Fauvelle, F., 2020. Beneficial effect of the hydroxychloroquine/azithromycin combination in elderly patients with COVID-19: Results of an observational study, the hospital pharmacist and clinician. 55, 398-403.
- [29] Chivese, T., Musa, A. H. O., Al-Wattary, N., Badran, S., Soliman, N., Ahmed, T. M. A., Joshua, M. T., Emara, M. M., Thalib, L., Doi, S. A. R., 2021. Efficacy of chloroquine and hydroxychloroquine in treating COVID-19 infection: A meta-review of systematic reviews and an updated meta-analysis Travel Medicine and Infectious Disease. 43, 102135. 5.
- [30] Hache, G., Rolain, J. M., Gautret, P., Deharo, J. C., Brouqui, P., Raoult, D., Honoré, S., 2021. Combination of Hydroxychloroquine Plus Azithromycin As Potential Treatment for COVID-19 Patients: Safety Profile, Drug Interactions, and Management of Toxicity. 27, 281-290.